www.czasopisma.pan.pl PAN www.journals.pan.pl
INTL JOURNAL OF ELECTRONICS AND TELECOMMUNICATIONS, 2014, VOL. 60, NO. 1, PP. 73–77
Manuscript received January 22, 2014; revised March, 2014. DOI: 10.2478/eletel-2014-0007

Fully Analytical Characterization of the Series Inductance of Tapered Integrated Inductors

Fábio Passos, M. Helena Fino, and Elisenda R. Moreno

***Abstract*—In this paper a general method for the determination of the series inductance of polygonal tapered inductors is presented. The value obtained can be integrated into any integrated inductor lumped element model, thus granting the overall characterization of the device and the evaluation of performance parameters such as the quality factor or the resonance frequency. In this work, the inductor is divided into several segments and the corresponding self and mutual inductances are calculated. In the end, results obtained for several working examples are compared against electromagnetic (EM) simulations are performed in order to check the validity of the model for square, hexagonal, octagonal and tapered inductors. The proposed method depends exclusively on the geometric characteristics of the inductor as well as the technological parameters. This allows its straight forward application to any inductor shape or technology.**

***Keywords*—inductor design, variable width integrated spiral inductors, CMOS analog integrated circuits, RF IC design**

I. Introduction

THE BENEFITS of wireless connections through radio frequency (RF), for both communications and data transmission, has been motivating research work in this field ever since Guglielmo Marconi sent the first radio signal across the Atlantic ocean in 1901 [1]. At the time the motivation was the ability of communicate with people at hundreds of kilometres away. Nowadays, the ability to communicate with people is taken for granted, and the main goal is now to increase the amount of information sent. To accomplish this goal, an increasing demand for bandwidth has pushed new standards in the wireless domain. These new standards evolved towards higher operating frequencies. Besides the importance of the increasing bandwidth, wireless transmission allows the elimination of a physical connection between receiver and transmitter, which is a key advantage in modern communication systems. With the explosive growth of the wireless communication market the demand for fully integrated single chip RF transceiver systems also increased. The demand for low-cost RF integrated circuits also increased during the last years and a tremendous interest has been generated in on-chip passive components. During the past few years design efforts were made with the goal of integrating passive components such as resistors, capacitors and inductors. Compared to resistors and capacitors which nowadays have several integrated options, with most implementations being easy to model and implement, considerable effort is still needed to design and model on-chip inductors.

Integrated inductors are commonly used in tuning, filtering and impedance matching. The general lack of accurate Spice like models, leads RF designers to design inductors through a time consuming process of EM simulation and silicon verification [2]–[4]. The design of integrated inductor involves the determination of correlated geometric parameters, thus making this process a candidate for optimization based design methodologies. The integration of electromagnetic simulators into optimization loops in order to calculate the performance parameters of an inductor, such as inductance, quality factor and self-resonance frequency (SRF), is a timely prohibitive solution. To overcome the above mentioned problem, designers usually adopt analytical solutions or inductor lumped-element models to use in Spice like simulations. The first lumped element circuit to model an inductor was used in 1980 [5]. Since that date several authors suggested many different circuits to model an inductor and to incorporate effects such as substrate losses, skin effect, proximity effects and eddy currents [6]–[8]. A survey about integrated inductor state-of-the-art can be found in [9]. It is possible to develop non-intuitive models that integrate several field effects thus providing a more accurate model, however a trade-off between simplicity and accuracy should be maintained, so a simple model such as the well known π-model [10], as shown in Fig. 1, may be used.

Our focus in this paper is the determination of an analytical expression for the evaluation of the series inductance, L_s, for integrated planar tapered inductors of any shape (square, hexagonal, octagonal). It should be noted that some developments have been proposed over this methodology but always for non-variable width integrated inductors [4], [11]. The other passive elements presented in the model represent physical effects and may be calculated through a series of formulas given in [11], [12]. The proposed analytical expressions for the series inductance rely exclusively on

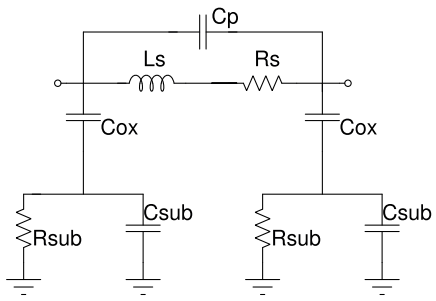

Fig. 1. Lumped-element inductor π-model.

F. Passos and M. H. Fino are with the New University of Lisbon, Faculty of Science and Technology, 2829-516 Caparica, Portugal, (e-mail: f.passos@campus.fct.unl.pt; hfino@fct.unl.pt).

E. R. Moreno is with the Institute of Microelectronics of Seville, CNM, CSIC and University of Seville, 41092 Seville, Spain, (e-mail: eli@imse-cnm.csic.es).

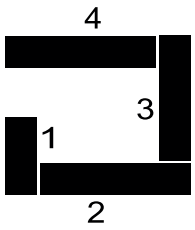

Fig. 2. Inductor model description for a one turn inductor.

geometric and technological parameters as a way of providing more physical insights into the design key parameters as well as enabling the straight forward application to new topologies and technologies.

The method used to characterize inductors in this work is based on the series inductance calculation, which is explained in Section II. Section III describes in detail the proposed modelling technique when applied to square, hexagonal and octogonal inductors. Section IV presents the advantages of using variable width inductors, and how to calculate the series inductance for this type of inductors. Section V present the experimental results against EM simulations, thus proving the validity of the model. Finally in Section VI conclusions and future work is presented.

II. Series Inductance

In 1929, Grover derived formulas for inductance calculation between filaments in several different relative positions [13]. Greenhouse later applied these formulas to calculate the inductance of a square shaped inductor by dividing the inductor into straight-line segments, as ilustrated in Fig. 2, and evaluating the inductance by adding up the self inductance of the individual segment and mutual inductance between segments [14]. Some authors call this method the *mutual inductance approach* [15].

For the inductor depicted in Fig. 2, the series inductance is given by (1). This specific case is the least complex one, where there are no mutual inductances between segments.

$$L_s = L_1 + L_2 + L_3 + L_4 \tag{1}$$

III. Polygonal Series Inductance Calculation

In this section the evaluation of the series inductance, L_s, for any n-side inductor is presented. For illustrative purposes, the particular case of an octagonal inductor is considered.

For an octagonal layout, such as the one in Fig. 3, the series inductance can be calculateb by (2).

$$L_s = L_0 + M_{p+} - M_{p-} - M_{lm} \tag{2}$$

where L_s is the total series inductance of the inductor, L_0 is the self inductance of each segment, M_{p+} is the parallel mutual inductance between segments where the current flows in the same direction whereas M_{p-} accounts for parallel mutual inductance where current flows in opposite directions, M_{lm} accounts for all the different types of mutual inductances

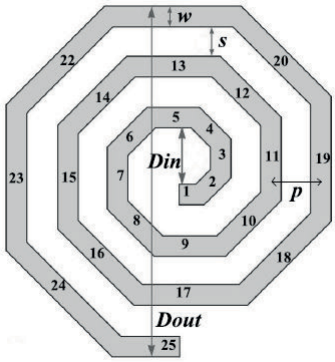

Fig. 3. Twenty-five section octagonal spiral inductor layout.

resulting from non-parallel segments. These mutual inductances should be added or subtracted depending on the relative flow of the current. The series inductance of the octagonal inductor depicted in Fig. 3 may be calculated with (3).

$$\begin{aligned} L_s = {} & L_1 + L_2 + ... + L_{25} \\ & \text{(Self inductance)} \\ & +2(M_{1,9}+M_{2,10}+M_{3,11}+M_{4,12}+M_{5,13}+M_{6,14}+...+M_{17,25}) \\ & \text{(Positive mutual inductances)} \\ & -2(M_{1,5}+M_{2,6}+M_{3,7}+M_{4,8}+M_{5,9}+M_{10,6}+...+M_{25,21}) \\ & \text{(Negative mutual inductances)} \\ & -2(M_{1,2}+M_{2,3}+M_{24,25}+...+M_{1,3}+M_{3,5}+M_{23,25}+ \\ & ...+M_{1,11}+M_{2,12}+...+M_{16,25}) \\ & \text{(Different mutual inductances)} \end{aligned} \tag{3}$$

where to calculate the self inductance of each segment, L_i, the following formula should be used,

$$L_i = 2l\left\{ln\left[\frac{2l}{w+t}\right] + 0.50049 + \frac{w+t}{3l}\right\}(nH) \tag{4}$$

where l is the segment length, w is the segment width and t is the segment thickness. This formula was proposed by Greenhouse and is suitable for integrated inductors [14]. For the evaluation of the mutual inductances, $M_{i,j}$, the relative positions of the segments must be taken into account. Due to the magnitude and phase of the currents, the mutual inductances are assumed identical in all sections, hence $M_{i,j}$=$M_{j,i}$.

For the evaluation of the mutual inductances, four different cases reflecting the relative positions of the segments must be considered: 1) between parallel segments, 2) between segments that are connected at one end, 3) between segments where the intersection point is lying outside the two segments and 4) between segments where the intersection point lies upon one segment. All these cases can be calculated with the formulas provided by Groover [13], as presented in the following sub-sections.

A. Parallel Segments

An example of two parallel segments is illustrated in Fig. 4 where l_i and l_j represent the segments lengths, p is the pitch

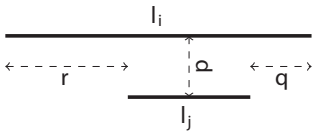

Fig. 4. Parallel segments.

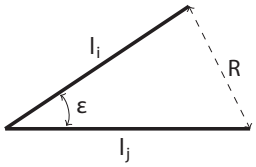

Fig. 5. Inductor segments connected at one end.

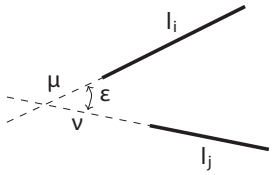

Fig. 6. Inductor segment intersection outside the two segments.

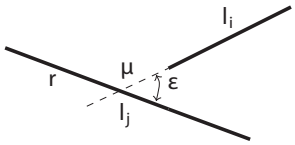

Fig. 7. Case for when the intersection point lies upon one segment.

of the two wires. The pitch, p, of the inductor, is the distance between the center of two parallel segments as can be observed in Fig. 3. On the other hand, r and q are the difference between the length of the segments. For the case of two parallel segments, as depicted in Fig. 4, the mutual inductances between two segments are calculated through the following equation.

$$M_{l_i,l_j} = 0.5 \cdot \left[(m_{l_j+r} + m_{l_j+q}) - (m_r + m_q)\right] \quad (5)$$

where each m_{l_x}, is given by,

$$m_{l_x} = 2 \cdot l_x \cdot U_x \quad (6)$$

When calculating m_{l_j+p} for example, in (6) the segment length l_x, should be equal to $l_j + p$. The mutual inductance factor, U, and can be calculated through (7).

$$U = ln\left[\frac{l_x}{d_x} + \sqrt{1+\left(\frac{l_x}{d_x}\right)^2}\right] - \sqrt{1+\left(\frac{d_x}{l_x}\right)^2} + \frac{d_x}{l_x} \quad (7)$$

where the distance between segments, d_x, is considered as the geometric mean distance (GMD), between segments and calculated by (8).

$$ln(d_x) = ln(p) - \frac{w^2}{12p^2} - \frac{w^4}{60p^4} - \frac{w^6}{168p^6} - \frac{w^8}{360p^8} - \frac{w^{10}}{660p^{10}} \quad (8)$$

where w is the width of the segments in study.

B. Segments which are Connected at One End

An example for mutual inductance for segments which are connected at one end, such as $M_{4,3}$, is presented in Fig. 5.

These types of mutual inductance are calculated through (9),

$$M_{l_i,l_j} = 2cos(\varepsilon) \cdot \left[l_i tanh^{-1}\left(\frac{l_j}{l_i+R}\right) + l_j tanh^{-1}\left(\frac{l_i}{l_j+R}\right)\right] \quad (9)$$

where l_i and l_j are the lengths of the segments and R is the distance between the segment ends, that can be calculated by (10).

$$R^2 = 2l_i^2(l_i - cos(\varepsilon)) \quad (10)$$

It is also possible to use one of the following relations to obtain either R or ε.

$$cos(\varepsilon) = \frac{l_i^2 + l_j^2 - R^2}{2l_i l_j} \quad (11)$$

$$\frac{R^2}{l_i^2} = 1 + \frac{l_j^2}{l_i^2} - 2\frac{l_j}{l_i}cos(\varepsilon) \quad (12)$$

C. Segments where the Intersection Point is Lying Outside the Two Segments

The case of mutual inductance where the intersection point is lying outside the two segments, for example, $M_{3,5}$ (in Fig. 3), is given in Fig. 6.

The mutual inductances in Fig. 6 are calculated by the following equation,

$$M_{l_i,l_j} = 2cos(\varepsilon) \left[(M_{\mu+l_i,\nu+l_j} + M_{\mu,\nu}) - (M_{\mu+l_i,\nu} + M_{\nu+l_j,\mu})\right] \quad (13)$$

where each one of the mutual inductances inside the parenthesis are calculated using (9).

D. Segments where the Intersection Point Lies upon One Segment

The case where the intersection point lies upon one segment, is the most complex case. An example of this type of mutual inductances is for example $M_{5,14}$ (in Fig. 3). This mutual inductance is presented in Fig. 7.

It is important to state that l_j is the entire segment. The mutual inductances in Fig. 7 are calculated by the following equation,

$$M_{l_i,l_j} = 2cos(\varepsilon) \left[(M_{l_i+\mu,l_j-r} + M_{l_j-r,\mu}) - (M_{l_i+\mu,r} + M_{r,\mu})\right] \quad (14)$$

where again, each one of the mutual inductances inside the parenthesis are calculated using (9). For the evaluation of the mutual inductances between segment l_i and r, and between $l_i + \mu$ and r an angle of $\pi - \varepsilon$ must be considered.

IV. Tapered Square Inductor

The design of an optimal spiral is highly frequency dependent. This is due to the multiple loss mechanisms that appear from the distributed effects in the structure. In general, for a fixed area, we can design an inductor with many different values of metal width w, spacing s, and turns n, to achieve the same value of inductance. As we increase w for instance, the resistance drops. This drop is proportional to $1/W$ at low frequencies but much more gradual at higher frequencies, due to the skin effect, especially with $w \gg \delta$, where δ is the effective skin $width$ [16]. The substrate losses, though, tend to increase with w, since this increases the parasitics. At the same time, we observe that structures with more turns, n, tend to have higher resistive losses in the inner turns. The origin of these enhanced losses is due to the fact that the magnetic flux increases as we move towards the center of the spiral, due to the additive nature of the flux from each successive loop of the spiral, for this reason hollow spirals are preferred [17]. If the width of the structure is tapered, as shown in Fig. 8, then the performance of the spiral can be improved [18]. Since the wide inner turns do not lower the resistance (due to current constriction), it is better to transfer the width to the outer turns, while keeping the total area of the spiral constant. For the optimum design of tapered inductors a general method for the characterizing its behaviour is needed.

The method proposed to calculate the series inductance of this tapered layout is exactly the same as it was for non tapered. A simple expression can be used to increase the width of each segment proportionately. This formula is the same one that ASITIC uses for the design the layout of tapered integrated inductors and is given by,

$$w_x^2 = w_0 + (w_i - w_0) \cdot \frac{x}{N_{sides} \cdot n} \tag{15}$$

where w_0 is the width of the last segment of the outer turn, whereas w_i stands for the first segment of the inner turn, x is the number of the segment, n is the number of turns and N_{sides} is the number of sides of the polygonal structure. However the width of each turn can be completely independent of any equation. However, a small consideration has to be taken into account. For tapered inductors, the pitch, p, in (8), is no longer constant. A tapered integrated inductor is depicted in Fig. 8.

V. Results and Discussion

In this section we present the results obtained for the evaluation of the series inductance with the proposed method. For the validation of the model we present results for square, hexagonal and octagonal inductors with non-variable width. The obtained results were compared against EM simulation with ADS Momentum [19]. The technology used for the simulation was UMC 130 nm. To reduce the losses, all inductors were implemented in the top most available layer, so in UMC 130 nm, metal 8 should be used, which has thickness, t of 2 um. The square inductors have an area of 350×350 μm^2 and the hexagonal and octagonal inductors have an area of 400×400 μm^2. All the inductors have a metal width, $w = 10\mu$m and a spacing between metals, $s = 2.5\mu$m. The error presented as ε_M, is the error of the model compared to EM simulation.

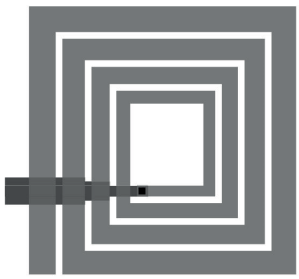

Fig. 8. A square spiral inductor with tapered trace width.

TABLE I
L_s Results with the Model Compared to EM ADS Momentum Simulations for Equal Width Inductors.

Sides	n	L_M	L_{ADS}	ε_M (%)
4	2	3.48	3.45	**0.99**
4	3	6.55	6.46	**1.39**
4	4	9.89	9.77	**1.23**
4	5	13.25	13.24	**0.08**
6	2	3.05	3.00	**3.15**
6	3	5.90	5.65	**4.44**
6	4	9.20	8.60	**6.98**
6	5	12.24	11.68	**7.96**
8	2	3.30	3.17	**4.10**
8	3	6.40	6.00	**6.67**
8	4	9.91	9.25	**7.14**
8	5	13.40	12.60	**6.35**

For square inductors we have typical errors of 2-3%. On the contrary of what was stated in other papers [12], it was possible to design hexagonal and octagonal inductors, with errors typically smaller than 2-3%. For smaller inductors the error percentage is slightly higher and the reason may be that for smaller inductors and for higher number of turns, the inductor stops being hollow, increasing the eddy currents which are not considered in this model.

For the tapered inductors, several simulations have been made for octagonal tapered width inductors. The results are presented in Tab. II. In this table the inductors simulated go from $n = 2$ until $n = 6$. Every inductor has the first turn width (w_1) equal to 14 μm and the last turn width equal to 20 μm. The variation between each turn is independent of any equation, but a ratio between each turn width was maintained and the area of all the inductors is the same.

The results presented for the tapered octagonal inductors have an average error around 2.5% which proves the validity of the proposed method even for the most difficult layout used nowadays. Square and hexagonal layouts have much less segments, therefore decreasing the complexity of the

TABLE II
L_s RESULTS WITH THE MODEL COMPARED TO EM ADS MOMENTUM SIMULATIONS FOR TAPERED WIDTH INDUCTORS.

n	D_{in}	w_1	w_2	w_3	w_4	w_5	w_6	Area	L_M	L_{EM}	Error
2	227	14	20	-	-	-	-	300	1.84	1.97	**6.41**
3	188	14	17	20	-	-	-	300	3.43	3.46	**0.84**
4	149	14	16	18	20	-	-	300	4.92	4.88	**0.84**
5	110	14	15.5	17	18.5	20	-	300	6.18	6.08	**1.66**
6	74	14	15	16	17	18.5	20	300	7.26	7.07	**2.69**

calculations, which is an indicator that the results would be even more accurate.

VI. CONCLUSION

In this paper we have introduced an efficient integrated inductor model for the prediction of the inductance for several integrated inductor layouts. The results have been compared with EM simulations with ADS Momentum where the model has proven its validity for the different layouts, with all results showing low deviations with respect to the EM simulations. It was also proven that this model is suitable for its usage with tapered inductors of different layouts. It may be observed that generally the model achieves average errors of 3 %, thus making this model a candidate for the design of integrated inductors. As future work, the idea is to integrate this inductance model into a pi lumped element model as a way of evaluating the other performance parameters related with integrated inductors, such as quality factor and self-resonance frequency. This way, in the future the model can be integrated in single- and multi-optimization algorithms in order to reduce time on the design of integrated inductors. Exploring new layouts for tapered inductors such as increasing the turn width in the first turns and then decrease the width can also be a topic for future research.

REFERENCES

[1] H. Zhang, "Quality factor enhanced coupled inductor structurs and their RF applications," *McGill University*, 2004.
[2] J. Rogers, D. Rahn, and C. Plett, "A 2.4GHz wide tuning range VCO with automatic level control circuitry," in *Proceedings of the 27th European Solid-State Circuits Conference*, September 2001, pp. 341–344.
[3] M. P. Wilson, "Modeling of itegrated vco resonators using momentum," in *technical paper, Agilent Technologies publication*, 2002.
[4] V. Blaschke and J. Victory, "A Scalable Model Methodology for Octagonal Differential and Single-Ended Inductors," in *IEEE Custom Integrated Circuits Conference*, September 2006, pp. 717–720, doi 10.1109/CICC.2006.320897.
[5] R. Rodriguez, J. Dishman, F. Dickens, and E. Whelan, "Modeling of Two-Dimensional Spiral Inductors," *IEEE Transactions on Components, Hybrids, and Manufacturing Technology*, vol. 3, no. 4, pp. 535–541, December 1980, ISSN 0148-6411, doi 10.1109/TCHMT.1980.1135651.
[6] A. M. Niknejad and R. G. Meyer, "Analysis, Design, and Optimization of Spiral Inductors and Transformers for Si RF IC's," *IEEE Journal of Solid-State Circuits*, vol. 33, pp. 1470–1481, 1998.
[7] F. M. Rotella, V. Blaschke, and D. Howard, "A broad-band scalable lumped-element inductor model using analytic expressions to incorporate skin effect, substrate loss, and proximity effect," in *Internationa Electron Devices Meeting*, 2002, pp. 471–474, doi 10.1109/IEDM.2002.1175881.
[8] Y. Cao, R. A. Groves, N. D. Zamdmer, J. Plouchart, R. A. Wachnik, X. Huang, T. King, and C. Hu, "Frequency-independent equivalent circuit model for on-chip spiral inductors," in *Proceedings of the IEEE Custom Integrated Circuits Conference*, 2002, pp. 217–220, doi 10.1109/CICC.2002.1012800.
[9] S. Arvas, "Spiral inductor model extraction: A survey of the field," in *IEEE 13th AnnualWireless and Microwave Technology Conference (WAMICON)*, April 2012, pp. 1–7, doi 10.1109/WAMICON.2012.6208479.
[10] K. B. Ashby, I. A. Koullias, W. C. Finley, J. J. Bastek, and S. Moinian, "High q inductors for wireless applications in a complementary silicon bipolar process," *IEEE Journal of Solid-State Circuits*, vol. 31, no. 1, pp. 4–9, January 1996, ISSN 0018-9200, doi 10.1109/4.485838.
[11] Y. K. Koutsoyannopoulos and Y. Papananos, "Systematic analysis and modeling of integrated inductors and transformers in RF IC design," *IEEE Transactions on Circuits and Systems II: Analog and Digital Signal Processing*, vol. 47, no. 8, pp. 699–713, August 2000, ISSN 1057-7130, doi 10.1109/82.861403.
[12] J. Chen and J. J. Liou, "On-Chip Spiral Inductors for RF Applications: An Overview," *Semiconductor Technology and Science*, vol. 4, pp. 149–167, 2004.
[13] F. W. Grover, "Inductance Calculations: Working Formulas and Tables," *Courier Dover Publications*, 1929.
[14] H. Greenhouse, "Design of planar rectangular microelectronic inductors," *IEEE Transaction on PHP*, vol. 10, no. 2, pp. 101–109, June 1974.
[15] I. Bahl, *Lumped Elements for RF and Microwave Circuits*. Artech House Boston, 2003.
[16] A. M. Niknekad, *Electromagnetics for High-Speed Analog and Digital Communication Circuits*. Cambridge University Press, 2007.
[17] J. Craninckx and M. S. J. Steyaert, "A 1.8-GHz low-phase-noise CMOS VCO using optimized hollow spiral inductors," *IEEE Journal of Solid-State Circuits*, vol. 32, no. 5, pp. 736–744, May 1997, ISSN 0018-9200.
[18] J. López-Villegas, J. Samitier, C. Cané, P. Losantos, and J. Bausells, "Improvement of the Quality Factor of RF Integrated Inductors by Layout Optimization," *IEEE Transactions on Microwave Theory and Techniques*, vol. 48, 2000.
[19] Momentum, ADS2002, "Agilent Technologies," *EEsof division, Santa Rosa, CA*, 2006.
[20] S. S. Mohan, M. Del Mar Hershenson, S. P. Boyd, and T. H. Lee, "Simple accurate expressions for planar spiral inductances," *IEEE Journal of Solid-State Circuits*, vol. 34, pp. 1419–1424, 1999.
[21] S. S. Mohan, "Simple accurate expressions for planar spiral inductances – Oral Presentation," 1999.
[22] C. Yue and S. Wong, "Physical modeling of spiral inductors on silicon," *IEEE Transactions on Electron Devices*, vol. 47, no. 3, pp. 560–568, March 2000, ISSN 00189383, doi 10.1109/16.824729, http://dx.doi.org/10.1109/16.824729.
[23] Y. Eo and W. R. Eisenstadt, "High speed VLSI interconnect modeling based on S-parameter measurements," *SRC Pub C93337*, July 1993.
[24] R. A. Pucel, D. J. Masse, and C. P. Hartwig, "Losses in microstrip," *IEEE Transactions on Microvawe Technology*, vol. 16, no. 6, pp. 342–350, 1968.
[25] ——, "Determination of coupling capacitance of underpasses, air bridges and crossings in MICs and MMICs," *Electronics Letters*, vol. 23, pp. 344–346, June 1968.
[26] K. B. Ashby, J. J. Bastek, and S. Moinian, "High Q inductors for wireless applications in a complementary silicon bipolar process," *IEEE Journal of Solid-State Circuits*, vol. 31, pp. 4–9, 1996.
[27] J. Burghartz, "Silicon RF Technology – The Two Generic Approaches," *Proceeding of the 27th European Solid-State Device Research Conference*, pp. 143–153, 1997.
[28] J. Zhao, "A new calculation for designing multilayer planar spiral inductors," *EDN*, vol. 55, pp. 37–40, July 2010.
[29] K. Boak, "An introduction to telephone line interfacing using the PIC microcontroller," http://puggy.symonds.net/čatalyticideas/rat_ring/index.
[30] J. O. Voorman, "Design and Applications of Adaptive Gyrators," *Solid State Circuits*, pp. 15–18, 1978.